Planetary waves: a numerical study of Rossby waves

Anna Lina P. Sjur and Jan-Adrian H. Kallmyr

December 14, 2018

Abstract

In this article, we study Rossby waves using different both implicit and explicit schemes for solving the wave equation numerically. We consider both the advantages and disadvantages of the methods, as well as their efficiency and accuracy. From this analysis, we find that the implicit scheme (centered) is more accurate and stable.

1 Introduction

We encounter wave phenomena everywhere in the natural sciences. From quantum mechanics to oceanography, we find that be it the motion of a particle or the ocean, we require knowledge of wave-like behaviour to solve the problem. In quantum mechanics, a particle's wave function is described by a complex-valued diffusion equation, the Schrödinger equation, while in oceanography, we can describe ocean waves using the wave equation,

$$\frac{\partial^2 u}{\partial x^2} = \frac{\partial^2 u}{\partial t^2}, \tag{1}$$

where x and t denote the spatial and temporal coordinates, respectively. The wave equation will be the topic of this paper, in particular, we will model Rossby waves, first identified by Rossby (1939). These are inertial, planetary waves in the Earth's atmosphere and ocean which motions contribute to extreme weather (Mann et al., 2017), might drive the El-Ninõ southern oscillation (ENSO) (Bosc and Delcroix, 2008), and is also produced by ENSO, see Battisti (1989). While we hope the reader appreciate the wide range of phenomena related to these waves, our article presents a numerical study of the waves isolated from other processes. We therefore begin by describing fundamental theory of waves and partial differential equations in the Theory section, present our algorithm and the technicalities relating to its implementation. In the Results section, we present our data as figures, before discussing their implications in the Discussion section. Concluding our paper, we present our final thoughts on the topic of simulating Rossby waves.

2 Theory

2.1 Wave analysis

Waves are solutions of the wave equation (see eq. 1), and have certain properties such as the phase velocity

$$c = \frac{\lambda}{T} = \frac{\omega}{k}, \tag{2}$$

where λ is the wavelength, T the period, ω the angular frequency and k the wavenumber. We found the phase velocity of a variety of waves graphically by studying Hovmöller diagrams (Hovmöller, 1949).

2.2 Rossby wave equation

Rossby waves are low frequency waves induced by the meridional variation of the Coriolis parameter f. This parameter depends on the rotation of the Earth Ω and the latitude φ, and is given by

$$f = \Omega \sin \varphi. \tag{3}$$

An approximation where f is set to vary linear in space is called the β-plane approximation, and can be written as

$$f = f_0 + \beta y, \tag{4}$$

where $\beta = \frac{df}{dy}\Big|_{\varphi_0} = \frac{2\Omega}{a}\cos\varphi_0$, a being the radius of the Earth. Combining the β-plane approximation with the shallow water vorticity equation, you get the quasi-geostrophic vorticity equation. This can be linearised, and by assuming a constant mean flow without bottom topography, you get the barotropic Rossby wave equation:

$$\left(\partial_t + U\partial_x\right)\nabla_H\psi + \beta\partial_x\psi = 0. \tag{5}$$

Here, ψ is the stream function describing the velocity perturbation, ∂_x denotes $\frac{\partial}{\partial x}$, ∇_H is the horizontal divergence $\partial x + \partial y$ and U is the mean velocity. In this report, we will assume no mean velocity, i.e. $U = 0$, in which case equation (5) simplifies to

$$\partial_t\nabla_H\psi + \beta\partial_x\psi = 0. \tag{6}$$

Two forms of boundaries will be examined in this report, that is periodic and constant boundaries. The first case can be used to describe an atmosphere that wraps around the earth, where the stream function is equal at the end-points. The latter case, where the stream function has a constant value at the boundaries, can be used to describe an ocean basin.

When extending the problem to two dimensions, we require that the stream function is constant at all boundaries for the bounded case. For the periodic case, the stream function should wrap around in the east-west direction, which corresponds to the x-direction, while being constant at the north and south boundaries, corresponding to the boundaries in the y-direction.

A possible solution to (6) in one dimension with periodic boundaries, where $x \in [0, L]$, is given by

$$\psi = A\cos\left(kx - \omega t\right), \tag{7}$$

where $k = \frac{2n\pi}{L}$ and $\omega = -\frac{\beta L}{2n\pi}$. The phase speed c can be calculated through the dispersion relation, given by

$$c = \frac{\omega L}{2n\pi} = -\beta\left(\frac{L}{2n\pi}\right)^2. \tag{8}$$

Since β is positive for all latitudes, the phase speed will be negative, implying that Rossby waves travels from east to west in a bounded domain.

The same problem, but with constant boundaries equal to zero, has the possible solution

$$\psi = A\sin\left(\frac{\pi n}{L}x\right)\cos\left(kx - \omega t\right), \tag{9}$$

with $k = \frac{L}{\pi n}$ and $\omega = -\frac{\beta}{2k}$. Here, the phase speed is given by

$$c = \frac{\omega L}{2n\pi} = -\frac{\beta}{4} \tag{10}$$

Again, the phase speed is negative. Equation (9) describes a cosine wave where the amplitude is dependent on the position, following a sine curve with zeros at the boundaries.

2.3 Discretisation and algorithm

Scaling eq. 6, we essentially wanted to solve two equations

$$\partial_t\zeta + \partial_x\psi = 0 \tag{11}$$

$$\nabla_H \psi = \zeta, \tag{12}$$

where the latter is Poisson's equation. In one dimension, equation (12) simplifies to

$$\partial_{xx}\psi = \zeta, \tag{13}$$

To discretise, we use the following schemes:

$$\partial_q f \approx \frac{f_{q+1} - f_q}{\Delta q}, \tag{14}$$

$$\partial_q f \approx \frac{f_{q+1} - f_{q-1}}{2\Delta q}, \tag{15}$$

$$\partial_{qq} f \approx \frac{f_{q+1} - 2f_q + f_{q-1}}{(\Delta q)^2}, \tag{16}$$

where f is arbitrary and q a general coordinate. Here eq. 14 is the explicit forward scheme, with a truncation error proportional to Δq, and eq. 15 the implicit centered scheme, with a truncation error propotional to Δq^2. Equation (16) does as well have a truncation error probational to Δq^2 Letting $t^n = n\Delta t$ and $x_j = j\Delta x$, eq. 11 becomes

$$\zeta_j^{n+1} = \zeta_j^n - \frac{\Delta t}{2\Delta x}\left(\psi_{j+1}^n - \psi_{j-1}^n\right) \tag{17}$$

in the explicit scheme, and

$$\zeta_j^{n+1} = \zeta_j^{n-1} - \frac{\Delta t}{\Delta x}\left(\psi_{j+1}^n - \psi_{j-1}^n\right) \tag{18}$$

in the implicit scheme. For Poisson's equation, we simply have

$$\frac{\psi_{j+1}^{n+1} - 2\psi_j^{n+1} + \psi_{j-1}^{n+1}}{(\Delta x)^2} = \zeta_j^{n+1}. \tag{19}$$

for one dimension. Our general algorithm is then Algorithm 1. What remains now is to determine how to solve the equations for closed and periodic boundary conditions. In the case of closed boundaries we had the Dirichlet boundary conditions, and could use gaussian elimination as outlined in one of our earlier papers (Sjur and Kallmyr, 2018). As for the

initialise ψ^0, ζ^0;
for $n = 0, 1, \ldots,\ T$ **do**
  for $j = 0, 1, \ldots, X$ **do**
    solve for ζ_j^{n+1} using explicit or implicit scheme;
  solve for ψ^{n+1} using Gaussian eliminatin or Jacobi's method;

Algorithm 1: Algorithm for solving the 1+1 dimensional Rossby wave equation. Here T and X are the grid sizes in the temporal and spatial dimensions respectively.

periodic domain, we found that the resulting matrix form of the Laplacian would be singular. This prompted us to implement Jacobi's method, as described by Hjorth-Jensen (2015).

Jacobi's method is an iterative method, involving making a guess for ψ_j^{n+1} for all j, and then, by rearranging Possion's equation, calculating ψ_j^{n+1}. The stream function is recalculated until the difference in ψ between two iterations is essentially zero.

Up until this point we had only considered the $1+1$ dimensional Rossby wave. Expanding to $2+1$ involves solving equation (12) using Jacobis method. Discretisising, the Possion equation in two dimensions becomes

$$\frac{\psi_{i,j+1}^{n+1} + \psi_{i+1,j}^{n+1} - 4\psi_{i,j}^{n+1} + \psi_{i,j-1}^{n+1} + \psi_{i-1,j}^{n+1}}{(\Delta x)^2} = \zeta_{i,j}^{n+1}, \tag{20}$$

given that $\Delta x = \Delta y$. Algorithm REF outlines the algorithm for solving the two-dimensional case.

2.4 Implementation

We implemented our algorithms in C++ using the armadillo and LAPACK libraries to handle matrix operations. To analyse data and produce figures, we used python 3.6 with a stan-

initialise ψ^0, ζ^0;
for $n = 0, 1, \ldots,\ T$ **do**
  for $j = 0, 1, \ldots, Y$ **do**
    for $i = 0, 1, \ldots, X$ **do**
      solve for $\zeta_{i,j}^{n+1}$ using explicit or implicit scheme;
  solve for ψ^{n+1} using Jacobi's method;

Algorithm 2: Algorithm for solving the 2+1 dimensional Rossby wave equation. Here T, X and Y are the grid sizes in the temporal and spatial dimensions respectively.

dard set of modules: matplotlib, numpy and seaborn.

3 Results

Looking at Figure 1, we observe the time evolution of a sine wave in the periodic domain. We see that the wave is easterly (travelling towards the west). There are four distinct anti-nodes throughout the entire duration of the wave, and a wavelength is determined to be 0.5. After a time $t = 80$ we can see that the wave is in phase to its initial state.

Considering now the bounded sine wave (Figure 2), the direction of propagation is still west. The shape of the curve appears to be the same as for the periodic case, except that the equilibrium line of the sine curve is shifting up and down, so that the boundary conditions are satisfied.

From Figure 3, 4 and 5, we see that, in general, the periodic gaussian wave exhibits different behaviour compared to the sine wave. There are at most two distinct anti-nodes at any point in time, and there looks to be a changing pattern in time, compared to the sine waves which always look the same. For varying width, σ, we see that the location of the anti-node are more concentrated in the middle

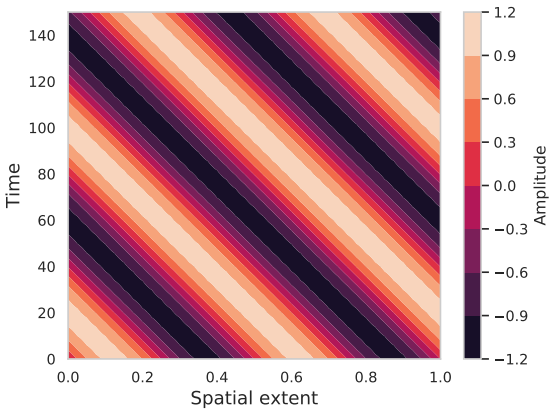

Figure 1: Hovmöller diagram of a Rossby wave with ***periodic*** *boundary conditions, initially a sine wave using a implicit scheme, where* $\Delta x = 0.025$ *and* $\Delta t = 0.1$.

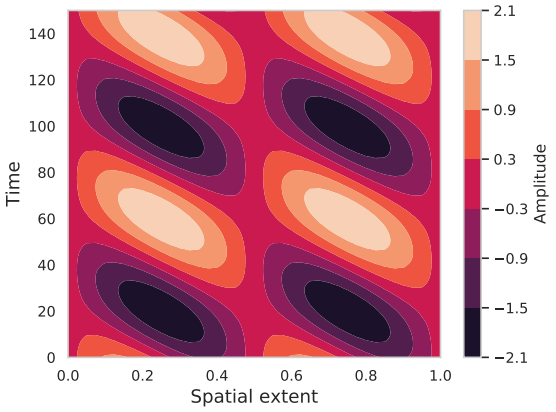

Figure 2: Hovmöller diagram of a ***bounded*** *Rossby wave with a initial sine wave using a implicit scheme. Here* $\Delta x = 0.025$ *and* $\Delta t = 0.1$.

for lower σ (Figure 3) and more spread out for higher σ (Figure 5).

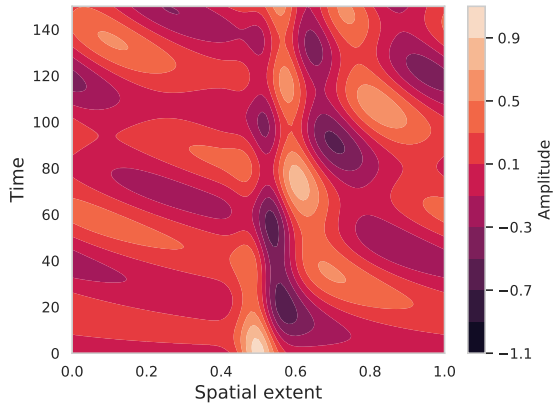

*Figure 3: Hovmöller diagram of a Rossby wave with **periodic** boundary conditions, initially a centered gaussian ($x_0 = 0.5$) using a implicit scheme. Here $\sigma = 0.05$, $\Delta x = 0.01$ and $\Delta t = 0.1$.*

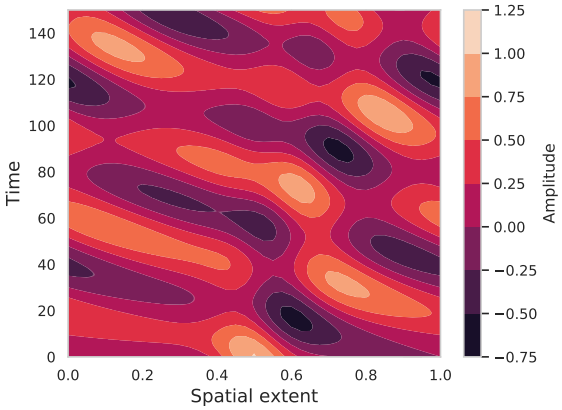

*Figure 4: Hovmöller diagram of a Rossby wave with **periodic** boundary conditions, initially a centered gaussian ($x_0 = 0.5$) using a implicit scheme. Here $\sigma = 0.1$, $\Delta x = 0.025$ and $\Delta t = 0.1$.*

In Figure 6 we show the Hovmöller diagram of a gaussian with closed boundaries. In this case, while there are still variations in time, we can clearly discern oscillations between minima and maxima.

Figure 8 and 7 shows the evolution of an initial product between two sine waves, one in the x-direction and one in the y-direction, resulting in an two dimensional wave, for four different time steps, both in a periodic and bounded domain. In the periodic domain, the wave seems to keep its structure, while shifting in the x-direction. The direction can not be derived solely from these four time steps. However, referring to the code for animating the time evolution found in the GitHub repository janadr/FYS3150/prosjekt5/kode, it can be seen that the wave is travelling to the left. It should be noted that due to a lack of time, the code used to generate the data shown in Figure 7 does not handle the eastward boundary correctly.

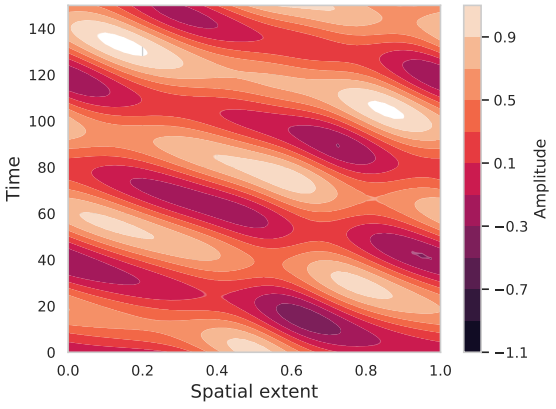

*Figure 5: Hovmöller diagram of a Rossby wave with **periodic** boundary conditions, initially a centered gaussian ($x_0 = 0.5$) using a implicit scheme. Here $\sigma = 0.15$, $\Delta x = 0.025$ and $\Delta t = 0.1$.*

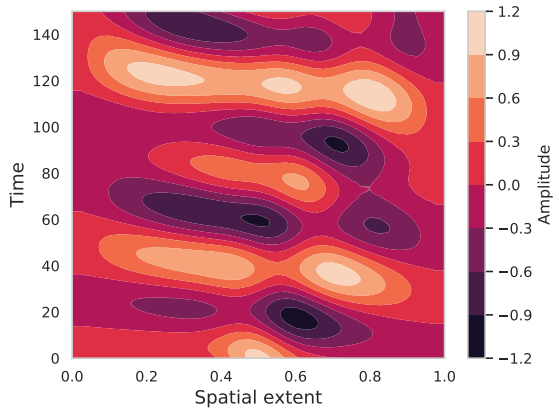

*Figure 6: Hovmöller diagram of a **bounded** Rossby wave initially a centered gaussian ($x_0 = 0.5$) using a implicit scheme. Here $\sigma = 0.1$, $\Delta x = 0.025$ and $\Delta t = 0.1$.*

For the bounded two dimensional domain, the amplitude of the wave have decreased closer to the x-boundaries for the time steps $t \neq 0$. Again it can be seen from the mentioned animation program that the wave is travelling westward.

4 Discussion

Looking back at the Hovmöller diagrams, we find that Figure 1 corresponds well with the analytical expression in eq. 7 as shown in the figure is the very distinct Hovmöller diagram for a cosine wave with a constant amplitude of 1. In the bounded case (Figure 2) we find that the amplitude oscillates with $\sin x$ as expected. Both waves are easterlies, which is as expected from the analytical negative dispersion relation (eq. 10), and correlates with Rossby's original observations (Rossby, 1939).

As for the gaussian waves, we have no analytical solutions, but find that

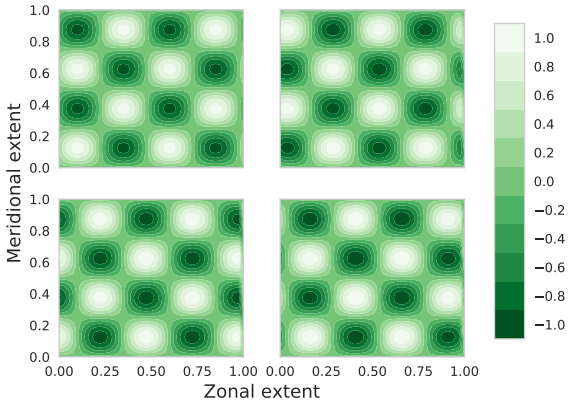

*Figure 7: 2+1 dimensional time evolution of a sine wave in the **periodic** domain, where time advances from left to right, top to bottom, for $t = 0, 50, 100, 150$ respectively. Here $\Delta x = 0.025$ and. $\Delta t = 0.1$*

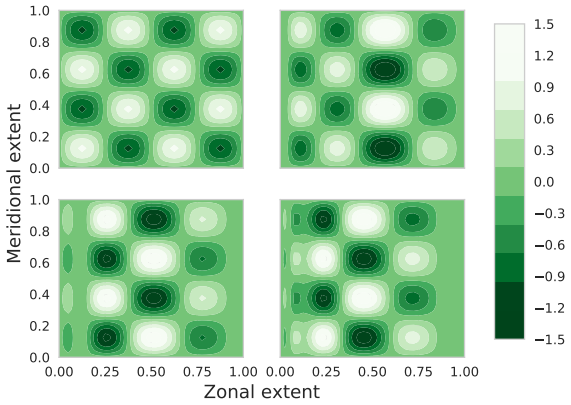

*Figure 8: 2+1 dimensional time evolution of a sine wave in the **bounded** domain, where time advances from left to right, top to bottom, for $t = 0, 50, 100, 150$ respectively. Here $\Delta x = 0.025$ and. $\Delta t = 0.1$*

5 Conclusion

References

David S Battisti. On the role of off-equatorial oceanic rossby waves during enso. *Journal of physical Oceanography*, 19(4):551–560, 1989.

Christelle Bosc and Thierry Delcroix. Observed equatorial rossby waves and enso-related warm water volume changes in the equatorial pacific ocean. *Journal of Geophysical Research: Oceans*, 113(C6), 2008.

Morten Hjorth-Jensen. Computational physics. https://github.com/CompPhysics/ComputationalPhysics/blob/master/doc/Lectures/lectures2015.pdf, 2015.

Ernest Hovmöller. The trough-and-ridge diagram. *Tellus*, 1(2):62–66, 1949.

Michael E Mann, Stefan Rahmstorf, Kai Kornhuber, Byron A Steinman, Sonya K Miller, and Dim Coumou. Influence of anthropogenic climate change on planetary wave resonance and extreme weather events. *Scientific Reports*, 7:45242, 2017.

Carl-Gustaf Rossby. Relation between variations in the intensity of the zonal circulation of the atmosphere and the displacements of the semi-permanent centers of action. *J. Mar. Res.*, 2:38–55, 1939.

Anna Lina P. Sjur and Jan-Adrian H. Kallmyr. Two methods of solving linear second-order differential equations. https://github.com/janadr/FYS3150/blob/master/prosjekt1/tex/main.pdf, 2018.

A

$$A = \begin{bmatrix} b_1 & c_1 & 0 & \dots & \dots & 0 \\ a_1 & b_2 & c_2 & 0 & \dots & 0 \\ 0 & a_2 & b_3 & c_3 & \dots & 0 \\ \vdots & \ddots & \ddots & \ddots & \ddots & \vdots \\ 0 & \dots & \ddots & a_{n-2} & b_{n-1} & c_{n-1} \\ 0 & \dots & \dots & 0 & a_{n-1} & b_n \end{bmatrix},$$